Tissue Repair Response as a Function of Dose in Thioacetamide Hepatotoxicity

Raja S. Mangipudy, Sanjay Chanda, and Harihara M. Mehendale

Division of Pharmacology and Toxicology, College of Pharmacy and Health Sciences, Northeast Louisiana University, Monroe, LA 71209-0470 USA

The purpose of the present study was to establish a dose–response relationship for thioacetamide (TA), where tissue regeneration as well as liver injury were two simultaneous but opposing responses. Male Sprague-Dawley rats were injected intraperitoneally with a 12-fold dose range of TA, and both liver injury and tissue repair were measured. Liver injury was assessed by serum enzyme elevations. Serum alanine aminotransferase (ALT) elevation did not show any dose response over a 12-fold dose range up to 24 hr. A dramatic ALT elevation was evident after 24 hr and only for the highest dose (600 mg/kg). Tissue regeneration response was measured by ^{3}H-thymidine (^{3}H-T) incorporation into hepatocellular DNA and by proliferating cell nuclear antigen (PCNA) procedure during a time course (6, 12, 24, 36, 48, 72, and 96 hr). Tissue regeneration, as indicated by ^{3}H-T incorporation, peaked at 36 hr after administration of a low dose of TA (50 mg/kg). With increasing doses, a greater but delayed stimulation of cell division was observed until a threshold was reached (300 mg/kg). Above the tissue repair threshold (600 mg/kg), because stimulated tissue repair as revealed by ^{3}H-T incorporation in hepatonuclear DNA was significantly delayed and attenuated, injury assessed by serum enzyme elevations was remarkably accelerated, indicating unrestrained progression of injury leading to animal death. These findings suggest that, in addition to the magnitude of tissue repair response, the time at which this occurs is critical in restraining the progression of injury, thereby determining the ultimate outcome of toxicity. Whereas dose-related stimulation of tissue repair leads to recovery, delayed and diminished tissue repair response at the high dose leads to progression of liver injury, leading to hepatic failure and animal death. These findings impact on the concept of employing maximally tolerated doses in cancer bioassays. Maximum tolerated doses might represent maximal stimulation of cell proliferation, thereby enhancing the likelihood of errors in DNA replication. Measuring tissue repair and injury as simultaneous biological responses to toxic agents might increase the usefulness of dose–response paradigms in predictive toxicology and in risk assessment.

Key words: dose response, maximally tolerated dose, mitosis, necrosis, proliferating cell nuclear antigen, thioacetamide, tissue repair. *Environ Health Perspect* 103:260–267 (1995)

A dose-response relationship that encompasses the characteristics of exposure and the spectrum of effects in a correlative manner is the most fundamental and pervasive concept of classic toxicology (*1*). Thioacetamide (TA), originally used as a fungicide, is a potent hepatotoxin which has been much studied since the first report of its toxic properties (*2–5*). Earlier literature (*6–8*) suggests that an obligate intermediate metabolite of TA that binds to proteins with the formation of acetylimidolysine derivatives (*9*) is responsible for TA-induced hepatotoxic effects (Fig. 1). TA stimulates DNA synthesis and mitosis in the liver of rats at doses that produce limited necrosis (*10,11*). The rise in DNA synthesis induced by TA follows a time sequence, which is similar to that seen after partial hepatectomy (*12*). Rats treated with 50 mg TA/kg body weight undergo hepatocellular proliferation as suggested by ^{3}H-thymidine (^{3}H-T) incorporation, which peaks 36 hr after administration (*10,13*).

We previously described an autoprotection model with TA (*14*). The mechanism of autoprotection is an adaptive response characterized by sustained and controlled hepatocyte proliferation, resulting in tissue repair that helps to overcome massive liver injury inflicted by the lethal dose. Tissue repair mechanisms and hepatocellular regeneration have been implicated in the ultimate outcome of toxicity after injury from a variety of chemicals including carbon tetrachloride (*15–19*) and acetaminophen (*20*). The emerging concept of all these studies is that, after infliction of injury, timely stimulation of tissue repair helps to restrain the progression of toxic injury leading to animal survival despite massive injury from a normally lethal dose. Interference with the tissue repair processes (*14,20–22*) leads to unrestrained progression of injury, culminating in sudden hepatic failure and death.

The preceding findings suggest that, in addition to inflicting tissue injury, toxic chemicals elicit a biological compensatory mechanism of tissue repair intended to overcome injury through tissue healing. Because stimulation of tissue repair appears to be a simultaneous biological response that accompanies injury, measuring this response in addition to quantifying injury might be helpful in fine-tuning the predictive value of dose–response relationships. Therefore, the objective of the present work was to test this hypothesis by developing a dose–response relationship where tissue repair and liver injury are two simultaneous but opposing responses to the administration of a 12-fold dose range of TA (50, 150, 300, and 600 mg/kg). Both tissue injury and tissue repair were measured during a time course (6, 12, 24, 36, 48, 72, and 96 hr) after the administration of TA. The findings of this study suggest that quantifying tissue injury and repair as two dynamic and opposing responses is likely to increase the predictive value of dose–response curves when they are included in dose–response paradigms.

Materials and Methods

Male Sprague-Dawley rats (175–225 g, 7–8 weeks old) were obtained from Harlan Sprague-Dawley Inc. (Indianapolis, Indiana) and were maintained over sawdust bedding free of any chemical contaminants for 10 days on a 12-hr photoperiod in our central animal facility. A temperature of 21 ± 1°C and 50% relative humidity were maintained at all times. The animals had free access to water and commercial rat chow (diet no. 7001; Teklad, Madison, Wisconsin) *ad libitum* before, during, and after treatment.

Thioacetamide (TA) and [^{3}H-methyl] thymidine (^{3}H-T, specific activity 1.7 Ci/mmol) were obtained from Sigma Chemical Co. (St. Louis, Missouri). The scintillation fluid (Scintiverse SX 16-4) was purchased from Fisher Scientific (Baton Rouge, Lousiana). All other biochemicals and chemicals were obtained from Sigma.

After an acclimation period, the rats were divided into four major groups and treated intraperitoneally with TA (50, 150, 300, and 600 mg/kg) dissolved in normal saline (0.9% NaCl). The respective controls received normal saline (1 ml/kg) as a vehicle for TA administration.

One experiment was designed to determine the lethality of TA in rats. After administering each dose of TA (50, 150,

Address correspondence to Harihara M. Mehendale, Division of Pharmacology and Toxicology, College of Pharmacy and Health Sciences, Northeast Louisiana University, Monroe, LA 71209-0470 USA.

Preliminary results of this study were presented at the fall meeting of the American Society for Pharmacology and Experimental Therapeutics, San Francisco and published in *Pharmacologist* [35:149 (1993)].

This work was supported by a starter grant from The Burroughs Wellcome Fund. We thank Harvey J. Clewell, senior project officer, ICF Kaiser International, Ruston, Louisiana, for helpful discussion and suggestions concerning the modeling approach.

Received 26 September 1994; accepted 7 December 1994.

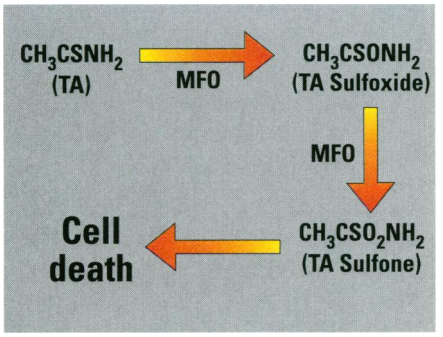

Figure 1. Mechanism of thioacetamide (TA) bioactivation leading to hepatotoxicity. MFO, mixed-function oxidase.

300, and 600 mg/kg), we observed the rats twice daily for 14 days, and survival/lethality was recorded in each group.

Blood was collected from the dorsal aorta of rats under diethyl ether anesthesia at 0, 12, 24, 36, 48, 72, and 96 hr after TA or vehicle administration, and the serum was separated to estimate the serum enzymes alanine aminotransferase (ALT; EC 2.6.1.2.) and sorbitol dehydrogenase (SDH; EC 1.1.1.14.) as markers of liver injury using kit no. 59 UV (ALT) and kit no. 50 UV (SDH), respectively, from Sigma.

Portions of liver from each group collected at various periods after TA treatment were washed with normal saline, cut into small slices, and fixed in phosphate-buffered 10% formaldehyde solution for 48 hr. Then the tissues were transferred to 70% ethyl alcohol until they were processed. After processing, these slices were embedded in paraffin. The liver sections (5 µm thick) were stained with hematoxylin–eosin (H&E) for histological examination under a light microscope.

We measured ^{3}H-T incorporation into hepatonuclear DNA using the procedure of Chang and Looney (*23*) as modified by Chauveau et al. (*24*). The DNA content of the supernatant fraction was estimated by the diphenylamine reaction (*25*).

The proliferating cell nuclear antigen study was conducted as described by Greenwell et al. (*26*). Briefly, the liver sections mounted on slides were first blocked with casein and then reacted with monoclonal antibody to PCNA (Dako Corporation, Carpentaria, California). The antibody was then linked with biotinylated goat anti-mouse IgG antibody (Boehringer/Mannheim, Indianapolis, Indiana), which was then labeled with streptavidin-conjugated peroxidase (Jackson Immunoresearch, West Grove, Pennsylvania). Color was developed by exposing the peroxidase-labeled streptavidin to diaminobenzidine, which forms a brown reaction product. The sections were then counterstained with Gill's hematoxylin. G_0 cells were blue and did not take the PCNA stain, G_1 cells were light brown in color, S-phase cell nuclei stained dark brown, and G_2 cells had cytoplasmic staining with or without a speckled nuclear appearance. We counted 1000 cells in each liver section.

Means ± SE were calculated for all values. Statistical differences were determined by one-way analysis of variance followed by Duncan's multiple range test to determine which means were significantly different from each other or from controls. In all cases, $p \leq 0.05$ was used as the statistical criterion to determine significant differences.

Results

Four groups of rats were treated with a 12-fold dose range of TA (50, 150, 300, and 600 mg/kg) and were observed for survival and lethality in each group for 14 days (Table 1). All rats in the groups receiving the sublethal doses of TA (50, 150, and 300 mg/kg) survived at the end of the 14 days, whereas the group receiving the lethal dose of 600 mg/kg experienced 100% lethality, with all deaths occurring between 4 and 7 days.

We estimated ALT as a marker of liver injury over time (0, 6, 12, 24, 36, 48, 72, and 96 hr). Figure 2 shows the serum enzyme activity at various times after the administration of each dose of TA. In the three groups receiving the sixfold dose range of TA (50, 150, and 300 mg/kg), enzyme levels increased initially and then declined to normal, indicating liver injury followed by recovery from that injury. The 100% animal survival in these three groups was consistent with the serum ALT elevation followed by decline. ALT elevation suggests that the injury inflicted by these three doses of TA was similar at 12 and 24 hr. At 24 hr, however, ALT elevation was similar in rats that received the full 12-fold dose range of TA. After 48 hr, liver injury in the rats that received the highest dose of 600 mg/kg progressed remarkably in an accelerated fashion, and all these rats died by 4–7 days. Thus, all rats receiving the sublethal doses (50, 150, or 300 mg/kg) survived, while the rats that received the 600 mg/kg dose did not survive. It should be noted that, because liver injury assessed by ALT elevation at 24 hr was similar across the full 12-fold range of doses, neither the extent of liver injury measured at one time point nor at multiple time points (e.g, 0 to 36 hr) predict the ultimate outcome of toxicity. The elevation of SDH, measured in a similar fashion, exhibited the same trend (data not shown).

Table 1. Fourteen-day lethality study after a single administration of thioacetamide[a]

Dose (mg/kg)	No. of rats	% Survival	% Lethality
50	10	100	0
150	10	100	0
300	10	100	0
600	10	0	100

[a]Route of administration for all the doses and saline controls was intraperitoneal. Thioacetamide was dissolved in normal saline (0.09% NaCl, 1 ml/kg). Rats were observed for 14 days, twice daily. All deaths occurred between days 4 and 7 after thioacetamide treatment.

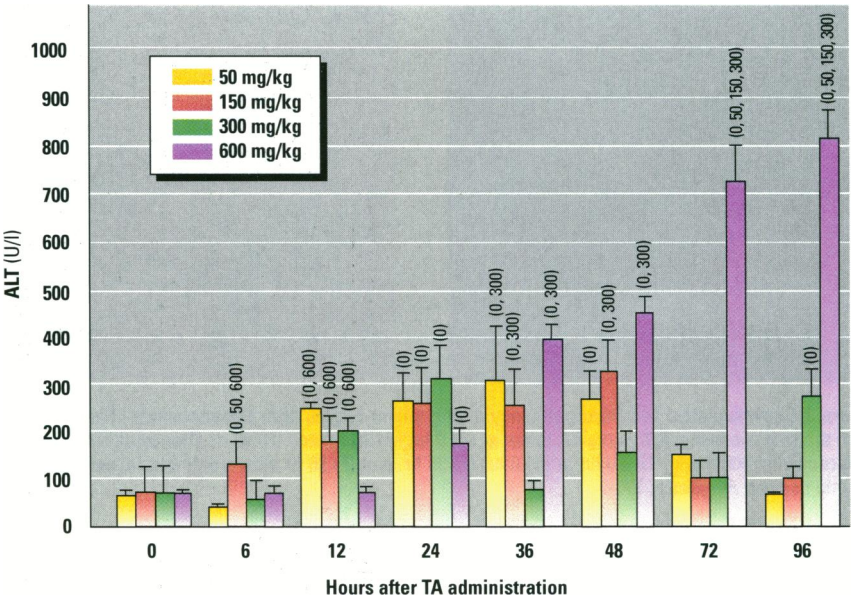

Figure 2. Male Sprague-Dawley rats (175–225 g) were divided into four groups. At time zero, the respective groups received intraperitoneal injections of 50, 150, 300, and 600 mg/kg thioacetamide (TA) in normal saline (1 ml/kg). Controls received normal saline (1 ml/kg). Serum alanine aminotransferase (ALT) was measured as a marker of liver injury over time (0, 6, 12, 24, 36, 48, 72, 96 hr) after each treatment. Results are expressed as means ± SE for four rats in each group. Numbers above error bars indicate significant differences from control (0 hr), 50, 150, 300, and 600 mg/kg treated groups, respectively ($p \leq 0.05$). Control ALT value: 54.3 U/l.

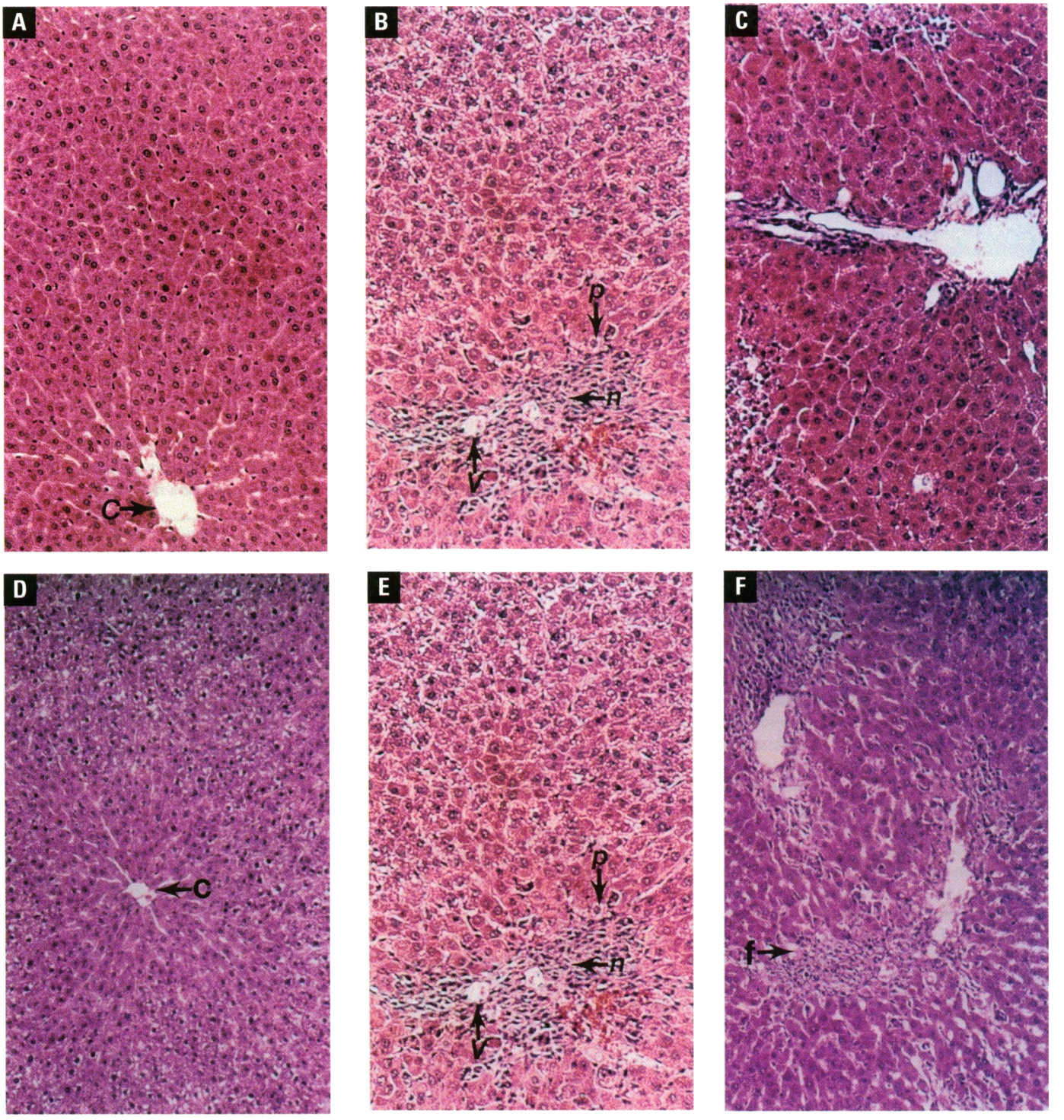

Figure 3. Representative liver histopathology during a time-course after thioacetamide (TA) treatment. Top panel represents photomicrographs of liver sections from the rats receiving 300 mg/kg TA taken at (A) 0 hr, (B) 36 hr, and (C) 96 hr after treatment. Bottom panel represents photomicrographs of liver sections from rats receiving 600 mg/kg TA taken at (D) 0 hr, (E) 36 hr, and (F) 96 hr after treatment. *c*, central vein; *p*, pyknotic nuclei; *v*, vacuolization; *n*, areas of necrosis; *f*, fibrotic tissues; *m*, mitosis; 100×.

We examined the liver sections stained by H&E for necrotic cells, extent of inflammation, neutrophil proliferation, and apoptotic bodies (Fig. 3). At 6 hr, centrilobular cells were slightly swollen in both the groups receiving 300 and 600 mg/kg TA, fine vacuoles had started appearing, and sometimes pyknotic nuclei were visible in a few cells. More distinct evidences of necrosis were visible at 12 hr, irrespective of the dose. The necrosed cells were concentrated around the central vein. The nuclei were somewhat larger in the necrosed cells, and the cells around the portal area were unaffected. Extensive centrilobular necrosis started at 24 hr for both 300 and 600 mg/kg groups. In the centrilobular area, liver-cell columns were broken up; the individual cells were separated from each other and appeared to be crumbling, indicating degeneration. The injury also started to spread toward the mid-zonal area. Some larger adjoining periportal tracts were damaged and necrosed. Necrosis was very prominent and almost the same for both groups between 36 and 48 hr. Between 72 and 96 hr, the peripor-

tal cells in the group receiving 300 mg/kg started showing active mitosis, in sharp contrast to increased widespread necrosis approaching the periportal area. Very little mitotic activity was seen in the group receiving 600 mg/kg.

Cell regenerative response indicated by S-phase DNA synthesis was found to peak between 36 and 48 hr in the group receiving the 300 mg/kg TA, but no such activity was noted in the group receiving 600 mg/kg during this time frame. Mitotic activity did appear in the group receiving the 600 mg/kg at 72 hr. However, it was much attenuated and delayed, leading to an unabated progression of injury resulting in death due to hepatic failure. With the 300 mg/kg TA treatment, however, presence of timely and adequate mitotic activity appeared to restrain the progression of injury, leading to recovery of animals from TA-induced hepatotoxicity.

Figure 4 illustrates incorporation of ^{3}H-T into hepatonuclear DNA over time following the administration of each dose of TA, measured as a marker of S-phase stimulation of cell cycle. Peak ^{3}H-T incorporation after the administration of 50 mg/kg occurred at 36 hr, whereas treatment with three-fold and six-fold higher doses resulted in peak ^{3}H-T incorporation at 48 hr. The magnitude of DNA synthesis due to the three- and six-fold higher sublethal doses was significantly higher. Nonetheless, this peak S-phase stimulation by a three-fold higher dose of 150 mg/kg was delayed 12 hr; it occurred at 48 hr after TA administration. With a six-fold higher dose of 300 mg/kg, although the peak DNA synthesis was also delayed by 12 hr and occurred at 48 hr, the increase included another additional increment in DNA synthesis. Treatment with the highest dose (600 mg/kg) however, resulted in an additional 24 hr delay and in a significantly attenuated S-phase synthesis of DNA. Therefore, in addition to being significantly delayed until 72 hr, the repair response was remarkably diminished. It was apparent that increase in TA dose leads to a dose-dependent temporal delay, and, beyond a threshold, a further increase in TA dose yields a diminished tissue repair response. It should be noted that at the maximally tolerated dose (MTD, 300 mg/kg), maximal S-phase stimulation was evident.

The results of ^{3}H-T incorporation (Fig. 4) were further corroborated by the PCNA immunohistochemical staining procedure (Figs. 5–7). Normally, most cells are in the resting phase (G_0; Fig. 6A), and a relatively small proportion of cells are in the other phases of cell cycle (Fig. 5), with about 3–4% in the G_2 phase. After the administration of TA (50 mg/kg), progression of G_2 cells to M phase (Fig. 5) was evident within 12 hr. Thereafter, continued cell cycle progression resulted in a large number of cells in G_1 at 24 hr, and in S phase at 36 hr. The maximum number of cells in S phase was seen at 36 hr (Fig. 5) by this method, in agreement with the peak of S-phase stimulation (^{3}H-T incorporation) observed at 36 hr after TA (50 mg/kg) administration. At 48 hr after the 50 mg/kg dose, most of the cells had progressed to the G_2 and M phases. By 96 hr, the liver returned to normal quiescence as evidenced by the predominant number of G_0 cells. With the 300 mg/kg group, a maximum number of cells were seen in S phase at 48 hr (Figs. 5 and 7B) after the administration of TA. This finding is commensurate with the results of ^{3}H-T incorporation studies (Fig. 4). At 72 hr after TA (300 mg/kg) treatment, most of the cells had progressed to the G_2 and M phase, indicating that cell cycle progression was

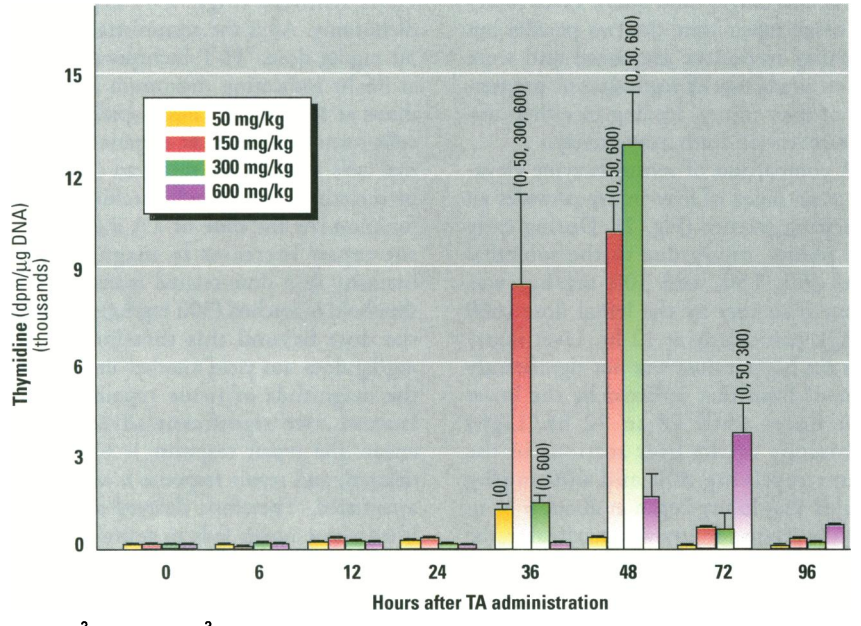

Figure 4. ^{3}H-thymidine (^{3}HT) incorporation into hepatonuclear DNA after thioacetamide treatment (TA). ^{3}H-T (35 µCi) was administered 2 hr before sacrifice at each time point. Results are expressed as means ± SE for four rats in each group. Numbers above error bars indicate significant differences from control (0 hr), 50, 150, 300, and 600 mg/kg treated groups, respectively ($p \leq 0.05$). Control ^{3}H-T value: 150.4 dpm/µg DNA.

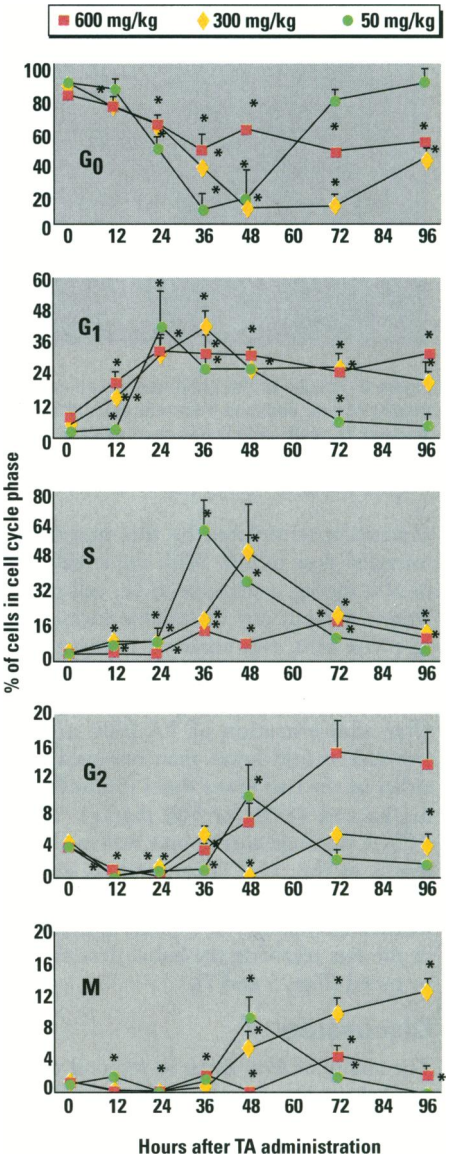

Figure 5. Graphical representation of cell cycle progression as measured by proliferating cell nuclear antigen, immunohistochemical procedure. Percentage was calculated from a total of 1000 viewed cells in the centrilobular region of the liver for each animal. Each time point had four rats per group. Rats received a single dose of 50, 300, or 600 mg/kg thioacetamide (TA), intraperitoneally. Percent cells in different phases of cell cycle were then counted during a time-course of 0–96 hr. (*)Significantly different from control ($p \leq 0.05$). Control rats received vehicle only (normal saline, 1 ml/kg, intraperitoneally).

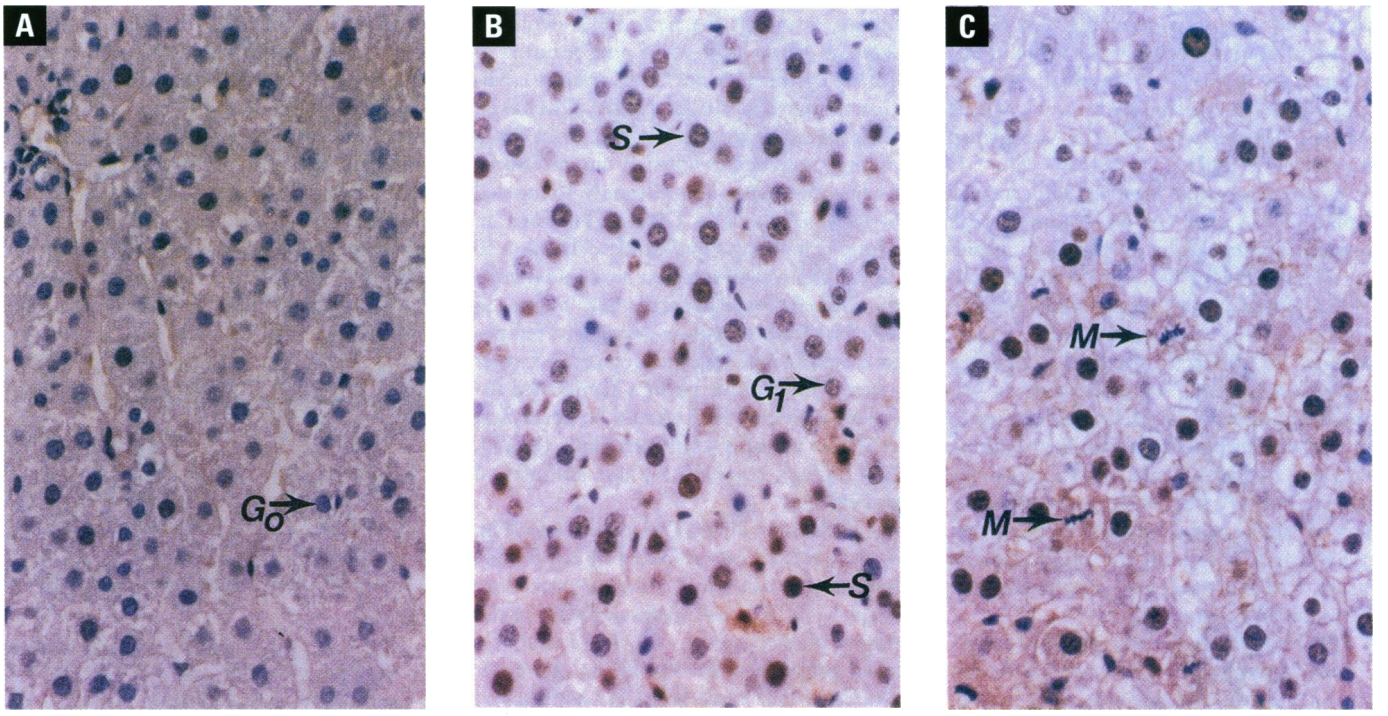

Figure 6. Results of the proliferating cell nuclear antigen study after intraperitoneal treatment with 50 mg/kg thioacetamide (TA). Representative photomicrographs of liver sections from rats at (A) 0 hr, (B) 36 hr, and (C) 48 hr after TA treatment. Details of treatment are described in text. G_0, cells with blue nuclear staining; G_1, cells with light-brown nuclear staining; S, cells with deep brown nuclear staining; G_2, cells with or without speckled nuclear staining and with diffused cytoplasmic staining; M, cells with diffuse cytoplasmic staining and with deep-blue chromosomal staining. Note significant S-phase stimulation at 36 hr and continuing cell cycle progression at 48 hr.

maximally stimulated by this maximally tolerated dose of TA. With the lethal dose of 600 mg/kg, a decrease in G_2 cell population, without any discernible increase in M-phase cells, was observed between 6 to 12 hr. The maximum number of cells seen in S phase at 72 hr (Fig. 5 and Fig. 7E) after administration of TA (600 mg/kg) was several fold lower than observed after either of the two lower doses (36 hr for 50 mg/kg and 48 hr for 300 mg/kg). These PCNA findings correspond well with the results of the ^{3}H-T incorporation studies. The remarkable delay in the onset and marked attenuation in S-phase stimulation in the rats receiving the lethal dose should be noted (Figs. 5 and 7).

Discussion

The ability of liver tissue to respond to tissue injury by stimulated hepatocellular regeneration has been demonstrated for TA (*13*), carbon tetrachloride (*16,17,27*), acetaminophen (*20*), and a number of additional structurally and mechanistically dissimilar chemicals (*27–30*). Tissue repair is a biological response that accompanies chemical-induced injury (*14,19,27,28*). Therefore, measuring this response in a dose–dependent and a temporal manner in parallel with injury may provide new insights on the use of dose–response relationships in predictive toxicology and risk assessment.

The objective of the present study was to test the hypothesis that quantifying tissue repair response along with injury in response to a toxic chemical should yield greater insight into the mechanism of toxicity on the one hand, and increase the usefulness of the standard dose–response paradigm on the other. Because these are two simultaneous dynamic events, they should be measured during a time-course rather than at one single time point. Liver injury and tissue repair were the two parallel but opposing responses measured and were used as predictors of regression or progression of liver injury, leading to either animal recovery or death, respectively.

A comparison of serum enzyme elevation as an index of liver injury provides an interesting picture (Fig. 2). During early time points, injury due to the sublethal doses (50, 150, and 300 mg/kg) was greater than that by the lethal dose (600 mg/kg), particularly at 12 hr. Liver injury from the highest dose was not significantly different from that inflicted by the lower three doses until 48 to 72 hr. Light microscopy of the liver sections in the groups receiving 300 and 600 mg/kg revealed that injury began at about 6 hr in both the groups. Injury was maximal in the group receiving 600 mg/kg between 36 and 48 hr, as evidenced by severe centrilobular necrosis, vacuolation, and congestion, while it was maximal between 24 and 36 hr in the group receiving the 300 mg/kg (Fig. 3). As expected, infiltration of polymorphonuclear cells was evident at this time as a mechanism for cleaning dead cells and tissue debris from the lobules. Thereafter, the rats receiving 600 mg/kg experienced remarkably accelerated progression of injury, whereas the rats receiving 50, 150, and 300 mg/kg experienced equally remarkable recovery from injury.

Tissue repair indicated by the S-phase DNA synthesis (Figs. 4–7) explains this dichotomy. After the administration of the 50 mg/kg dose, ^{3}H-T incorporation peaks at 36 hr indicating maximum DNA synthesis at this point. These rapidly dividing cells form new resilient hepatic parenchymal cells that replace the dead cells, thereby restoring hepatolobular architecture and function. As the dose of TA increases, tissue repair increases in magnitude and intensity in a dose-related manner until a threshold is reached (300 mg/kg). Increasing the dose beyond this threshold to 600 mg/kg does not yield another increment in the magnitude of tissue repair response. Instead, two significant adverse events ensue: the repair response is significantly delayed, and repair response is significantly attenuated. Therefore, delayed and diminished tissue repair fails to restrain the progression of liver injury (600 mg/kg), while prompt and adequate repair response aids in regression of liver injury and animal recovery (50, 150, and 300 mg/kg) through restored hepatic structure and function.

The progressive phase of injury due to the 600 mg/kg treatment is evident only

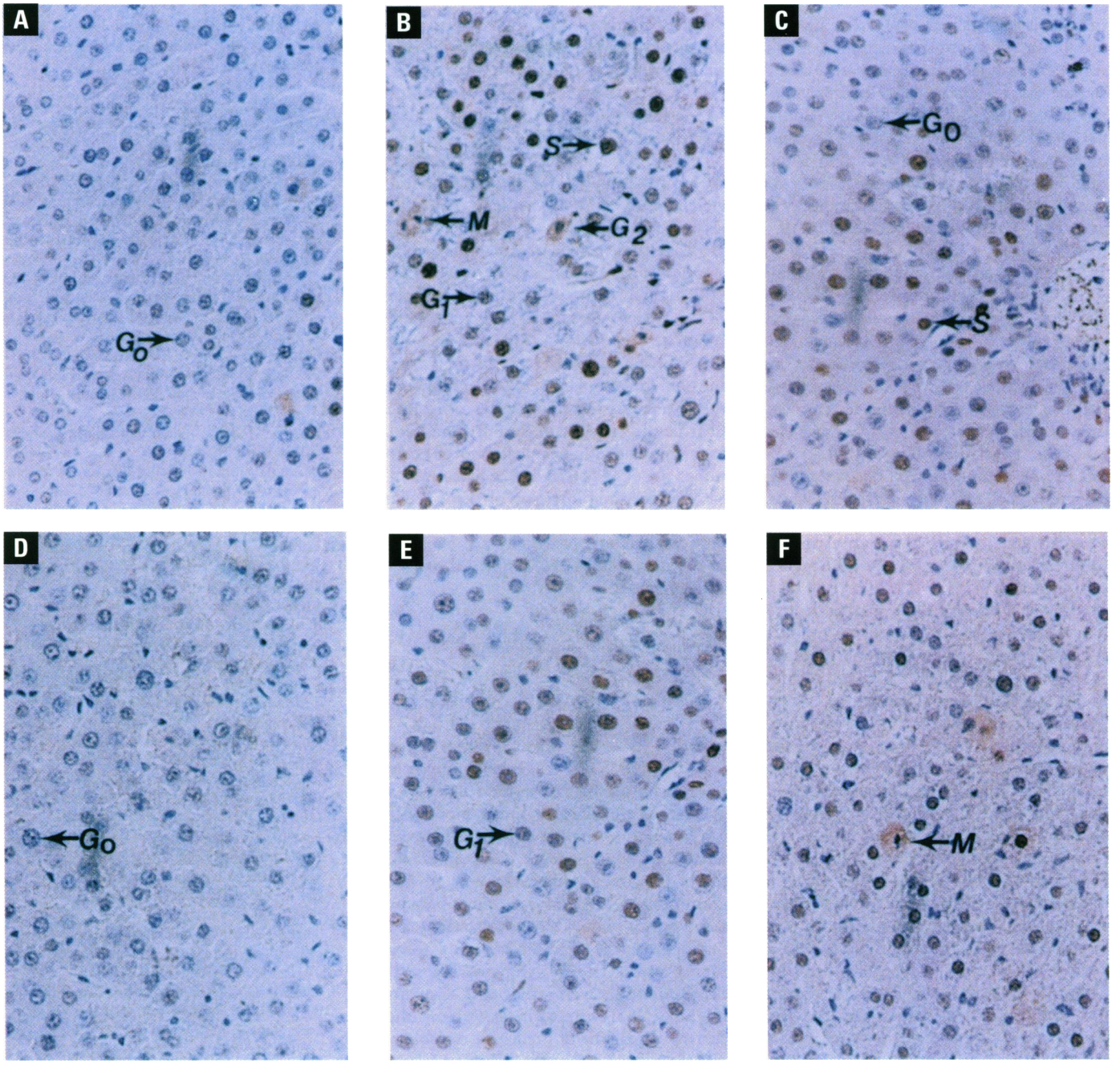

Figure 7. Results of the proliferating cell nuclear antigen study after intraperitoneal treatment with 300 and 600 mg/kg thioacetamide (TA). Representative photomicrographs of liver sections from rats at (A) 0 hr, (B) 48 hr, and (C) 72 hr after TA (300 mg/kg) treatment and (D) 0 hr, (E), 72 hr and (F) 96 hr after the higher dose of TA (600 mg/kg). Details of treatment are described in text. G_0, cells with blue nuclear staining; G_1, cells with light-brown nuclear staining; S, cells with deep-brown nuclear staining; G_2, cells with or without speckled nuclear staining and with diffused cytoplasmic staining; M, cells with diffuse cytoplasmic staining and with deep-blue chromosomal staining. Significant S-phase stimulation with 300 mg TA/kg (B) is contrasted with remarkably attenuated and delayed S-phase stimulation with 600 mg TA/kg (E).

after 48 hr when a dose-related increase in tissue repair fails to manifest. Therefore, the appearance of liver injury is not dose-related until after failure in exacting tissue repair is evident. At 12 hr, injury due to a 6-fold dose-range is the same, while at 24 hr there is no difference in injury due to a 12-fold dose-range. This is significant because it is inconsistent with the widely accepted paradigm of "high dose yielding greater metabolic activation" and therefore higher toxicity. If this were true, greater liver injury commensurate with the higher dose should have been evident during the first 36 hr, but this does not occur. Although the mechanism underlying this observation merits experimental validation, a possible explanation is worthy of consideration. Because the mechanism of TA hepatotoxicity is via the formation of a sulfoxide, which is thought to be metabolized to the reactive metabolite TA sulfone, it is possible that a dose of 600 mg/kg of TA also exerts an inhibition on the metabolism of TA sulfoxide to the reactive sulfone. This may happen because, after intraperitoneal administration, high levels of TA are achieved rapidly and are then subsequently metabolized via the mixed function oxidases to TA sulfoxide (*31*). However, because the subsequent metabolism of the sulfoxide to the reactive metabolite TA sulfone is also mediated by the same enzyme system(s), the relatively high levels of TA, following a 600 mg/kg dose, may inhibit the formation of the reactive species. Examples of substrate inhibition mechanism are available in the published literature. Thiobenzamide, a closely related aryl struc-

tural analog of TA, was shown to inhibit the metabolism of thiobenzamide sulfoxide to a reactive intermediate as the dose of thiobenzamide was increased (*32*). Another example of such inhibition of bioactivation is provided by the inhibition of benzene metabolism by phenol (*33*). Although this mechanism needs further scrutiny, it offers a logical explanation for insignificant injury at early time points after administration of a high dose.

Another fascinating observation of this study is the dynamic relationship between the tissue repair response and the progression of injury. It is only after failure to elicit a prompt tissue repair response that an accelerated progression of liver injury becomes evident, culminating in liver failure and death. Tissue repair due to a sixfold dose range peaks between 24 and 48 hr (Fig. 7), although with 600 mg/kg, it is delayed and significantly decreased. Thus, a failure in timely and adequate appearance of tissue repair leads to an unrestrained progression of injury in the 600 mg/kg treated group.

These findings have a potentially remarkable impact on the way we conduct risk assessment and predictive toxicology to protect environmental and public health. Significant advances in the understanding of mechanisms by which toxic chemicals inflict injury enable us to predict with a degree of confidence that a given toxic chemical or physical agent will or will not inflict tissue injury under a given set of exposure circumstances. However, the finding that the ultimate outcome of that injury is a result of the dynamic and opposing interaction between two biological responses, inflicted tissue injury and stimulated tissue repair, suggests that a greater understanding of the underlying biology is essential before achieving greater precision in predictive toxicology and risk assessment. Of immediate relevance in this regard are two important considerations. At least two levels of threshold doses can be suggested. One threshold exists for mechanisms, above which cell necrosis will occur (*28*) and tissue repair is stimulated. A second, higher threshold dose exists, above which the biological compensatory response of cell division and tissue repair are compromised in two distinct ways: a significant latency in stimulating the tissue repair response, and a significantly diminished response. The inevitable combined effect of this compromise is the unrestrained progression of tissue injury.

In between the two threshold doses, there is a dose-related incremental biological compensatory mechanism that effectively restrains tissue injury, permitting recovery from tissue injury. As stimulated cell division and tissue repair are the foundations of the biological compensatory response (*28,29*), this observation suggests the possibility of therapeutic intervention (*28*) in overcoming tissue injury, regardless of the mechanism or the extent of initial infliction of that injury.

Another consideration is the ongoing debate on the concept of the maximally tolerated dose (MTD) used in long-term studies such as cancer bioassays (*34,35*). MTDs are likely to maximally stimulate cell proliferation. In our present acute toxicity study, 300 mg TA/kg is likely to represent the MTD, a dose associated with maximally stimulated cell division. Repeated exposure to the MTD is likely to result in greater number of errors in DNA replication, thereby increasing the chances of cancer. Our findings may provide mechanistic basis for a scientific reevaluation of the continued use of MTDs in cancer bioassays.

The dynamic interplay of tissue repair and injury responses in determining the ultimate outcome of toxicity can be stated in a biologically based, empirical mathematical model:

$$\text{Outcome} = f(\text{Repair, injury})$$

$$\text{Outcome} = \{\text{Repair}(t) - \text{Injury}(t)\}dt$$

$$\text{Outcome} = \{\text{Repair}(t) \times W_r(t) - \text{Injury}(t) \times W_i(t)\}\text{dt}$$

where $W_r(t)$ is the weight given to repair (cell division), $W_i(t)$ is the weight given to injury (cell death). We suggest that, for a given dose, the ultimate outcome of injury is a function of the net difference between repair and injury, and that this difference can be integrated. This model may provide greater precision in risk assessment because this model is biologically based and it takes into account the dynamic nature of tissue repair and tissue healing processes. If experimentally validated, this concept might be more useful in improving the current paradigms of predictive toxicology and the science behind it. We plan to test this model in our future experiments.

References

1. Klaassen CD, Eaton DL. Principles of toxicology. In: Toxicology—the basic science of poisons, 4th eds (Klaassen CD, Amdur MO, Doull J, eds). New York:Pergamon Press, 1991;12–47.
2. Fitzhugh OG, Nelson AA. Liver tumors in rats fed thiourea or thioacetamide. Science 108:626–628 (1948).
3. Gallagher CH, Gupta DN, Judah JD, Rees KR. Biochemical changes in liver in acute thioacetamide intoxication. J Pathol Bact 72:193–201 (1956)
4. Gupta DN. Acute changes in the liver after administration of thioacetamide. J Pathol Bact 72:183–192 (1956).
5. Trennery PN, Waring RH. Early changes in thioacetamide induced liver damage. Toxicol Lett 19:299–307 (1983).
6. Becker V, Walter S. Die wirking von thioacetylverbindungen auf das leberparenchym im Tierexperiment. Acta Hepato-Solenol 12:129–140 (1965).
7. Ammon R, Berninger H, Haas HJ, Landsherg I. Thioacetamide sulfoxid, ein stoffwechsel produkt des thioacetamids. Arzneimittel Forschung 17:521–523 (1967).
8. Vadi HV, Neal RA. Microsomal activation of thioacetamide-S-oxide to a metabolite(s) that covalently binds to calf thymus DNA and other polynucleotides. Chem-Biol Interact 35:25–38 (1981).
9. Dyroff MC, Neal RA. Identification of the major protein adduct formed in rat liver after thioacetamide administration. Cancer Res 41:3430–3435 (1981).
10. Marley CGD, Boyer JL. Stimulation of hepatocellular proliferation by a serum factor from thioacetamide treated rats. Biochim Biophys Acta 477:165–176 (1977).
11. Diaz-Gil JJ, Sanchez G, Santamaria L, Trilla C, Esteban P, Escartin P, Gea T. A liver DNA synthesis promoter induced in rat plasma by injection of dimethylnitrosamine (DMNA) or thioacetamide. Br J Cancer 55:599–604 (1987).
12. Bucher NLR, Malt RA. Regeneration of liver and kidney, 1st ed. Boston:Little, Brown and Co., 1973;55–72.
13. Reddy J, Chiga M, Svoboda D. Initiation of division cycle of rat hepatocytes following a single injection of thioacetamide. Lab Invest 20:405–411 (1969).
14. Mangipudy RS, Chanda S, Mehendale HM. Thioacetamide autoprotection. FASEB J A40:225 (1993).
15. Kodavanti PRS, Joshi UM, Young RA, Bell AN, Mehendale HM. Role of hepatocellular regeneration in chlordecone potentiated hepatotoxicity of CCl_4. Arch Toxicol 6:367–375 (1989a).
16. Kodavanti PRS, Joshi UM, Young RA, Meydrech EF, Mehendale HM. Protection of hepatotoxic and lethal effects of CCl_4 by partial hepatectomy. Toxicol Pathol 17:494–505 (1989).
17. Thakore KN, Mehendale HM. Role of hepatocellular regeneration in CCl_4 autoprotection. Toxicol Pathol 19:47–58 (1991).
18. Thakore KN, Mehendale HM. Effect of phenobarbital and mirex pretreatment on CCl_4 autoprotection. Toxicol Pathol 22:291–299 (1994).
19. Calabrese EJ, Baldwin LA, Mehendale HM. Contemporary issues in toxicology. G_2 subpopulation in rat liver induced into mitosis by low level exposure to carbon tetrachloride: an adaptive response. Toxicol Appl Pharmacol 121:1–7 (1993).
20. Chanda S, Mangipudy RS, Warbritton A, Bucci TJ, Mehendale HM. Stimulated hepatic tissue repair underlies heteroprotection by thioacetamide against acetaminophen induced lethality. Hepatology 21:477–486 (1995).
21. Rao VC, Mehendale HM. Colchicine antimitosis abolishes CCl_4 autoprotection. Toxicol Pathol 19:597–606 (1991).
22. Rao VC, Mehendale HM. Effect of antimitotic agent colchicine on carbon tetrachloride toxicity. Arch Toxicol 67:392–400 (1993).
23. Chang LO, Looney WB. A biochemical and autoradiographic study of the in vivo utilization of tritiated thymidine in regenerating rat liver. Cancer Res 25:1817–1822 (1965).
24. Chauveau J, Moule Y, Roniller CH. Isolation of pure and unaltered liver nuclei morphology

and biochemical composition. Exp Cell Res 11:317–321 (1956).
25. Burton K. A study of the conditions and mechanisms of the diphenylamine reaction for positive colorimetric estimation of DNA. Biochem J 62:315–323 (1956).
26. Greenwell A, Foley JF, Maronpot RR. An enhancement method for immunohistochemical staining of proliferating cell nuclear antigen in archival tissues. Cancer Lett 54:251–256 (1991).
27. Nakata R, Tsukamoto I, Miyoshi M, Kojo S. Liver regeneration after intoxication in the rat. Biochem Pharmacol 34:586–588 (1985).
28. Mehendale, HM. Commentary: role of hepatocellular regeneration and hepatolobular healing in final outcome of liver injury. A two stage model of toxicity. Biochem Pharmacol 42:1155–1162 (1991).
29. Mehendale HM. Amplified interactive toxicity of chemicals at nontoxic levels: mechanistic consideration and implication to public health. Environ Health Perspect 102(suppl 9):139–149 (1994).
30. Zieve L, Anderson WR, Lyftogt C, Draves K. Hepatic regenerative enzyme activity after pericentral and periportal lobular toxic injury. Toxicol Appl Pharmacol 86:147–158 (1986)
31. Porter WR, Gudzinowicz MJ, Neal RA. Thioacetamide-induced hepatic necrosis. II. Pharmacokinetics of thioacetamide and thioacetamide S-oxide in the rat. J Pharmacol Exp Ther 208:386–391 (1979).
32. Scott JG, Darryl HP, Douglas K, Peter FS, Eugene GH, John GD, Anthony GZ. Thiobenzamide-induced hepatotoxicity: effects of substituents and route of administration on the nature and extent of liver injury. Toxicol Appl Pharmacol 111:388–408 (1991).
33. Schlosser PM, Bond JA, Medinsky MA. Benzene and phenol metabolism by mouse and rat liver microsomes. Carcinogenesis 14:2477–2486 (1993).
34. Ames BN, Gold LS. Chemical carcinogenesis: too many rodent carcinogens. Proc Natl Acad Sci USA 87:7772–7776 (1990).
35. Clayson DB, Iverson F, Mueller R. An appreciation of the maximum tolerated doses: an inadequately precise decision point in designing a carcinogenesis bioassay? Teratog Carcinog Mutagen 11:279–296 (1991).